Self-Assembled Monolayers of Tetrathiafulvalene Derivatives on Au(111): Organization and Electrical Properties †

ARTICLE *in* THE JOURNAL OF PHYSICAL CHEMISTRY B · APRIL 2004

Impact Factor: 3.3 · DOI: 10.1021/jp0495949

7 AUTHORS, INCLUDING:

Concepcio. Rovira
Spanish National Research Council
528 PUBLICATIONS **9,036** CITATIONS
SEE PROFILE

David B Amabilino
University of Nottingham
232 PUBLICATIONS **6,076** CITATIONS
SEE PROFILE

Self-Assembled Monolayers of Tetrathiafulvalene Derivatives on Au(111): Organization and Electrical Properties†

Elba Gomar-Nadal,‡ Ganesh K. Ramachandran,||,⊥ Fan Chen,|| Timothy Burgin,|| Concepció Rovira,‡ David B. Amabilino,*,‡ and Stuart M. Lindsay*,||

Institut de Ciència de Materials de Barcelona (CSIC), Campus de la UAB, 08193-Bellaterra, Spain, and Department of Physics and Astronomy, Arizona State University, Tempe, Arizona 85287

Received: January 29, 2004; In Final Form: March 18, 2004

Self-assembled monolayers (SAMs) formed by dissymmetric tetrathiafulvalene (TTF) derivatives on gold (111) are prepared, and the structural and electrical properties have been studied. The TTFs are united to the metal through two S−Au bonds while the other "end" bears two long alkyl chains. Observations based on a combination of surface characterization techniques including ellipsometry, FTIR, contact angle, STM, and AFM suggest that these monolayers are disordered or at least loosely packed in the lateral dimensions. Conduction through these molecular SAMs is remarkably high given that the length of the "insulating" alkyl chains attached to the TTF unit is on the order of 15−20 Å, a situation that arises in part from the tilted orientation of the molecules with respect to the surface and the loosely packed structure of the alkyl chains. Currents rivaling those in conjugated candidate "molecular wires" such as carotene dithiols and oligo-phenylene-ethynylenes are observed. The resistance of a single molecule in a SAM, determined in a two-terminal geometry using c-AFM, is estimated to be 25.7 ± 0.3 GΩ.

Introduction

The understanding of electronic conduction through and between organic molecules is of fundamental importance in molecular electronics,[1−4] electrochemistry,[5] and biochemistry.[6−7] To address and access the electronic properties of these molecules, a suitable organization method is necessary. Self-assembly of appropriately substituted molecules on metals is a general technique to deposit molecules in a monolayer.[8,9] One of our objectives is to adsorb and address redox-active organic molecules on surfaces, and to self-assemble systems comprised of these molecules. Tetrathiafulvalene (TTF) derivatives are ideally suited as components in this type of system because they are reversible and stable electron donors.[10,11] Their cation mixed valence radical salts represent an important class of conducting molecular materials,[12,13] and they have been incorporated as units in molecular machines.[14−15]

In this work, we report a new self-assembled monolayer (SAM) formed by tethering TTF derivatives through two thiolate groups directly to a gold surface (Scheme 1). The chemistry is tailored such that the Au−S− bond is linked directly to the TTF group, rather than being connected as a terminal group to an alkanethiol bonded to the gold surface. This indirect linkage was most common in previous studies on the self-assembly of molecules incorporating TTF units on metals.[16−23] We have employed a wide range of characterization techniques including ellipsometry, Fourier transform infrared spectroscopy (FTIR), contact angle, scanning tunneling microscopy (STM), and atomic force microscopy (AFM) to characterize these monolayers. Electron transport measurements through the TTF molecules have been carried out at controlled forces in a two-terminal geometry using a metal-coated conducting atomic force microscope (c-AFM).

SCHEME 1: Preparation of Dithiolates 1 and 2, a Schematic Description of the SAM Formation Process, and a Cartoon of the SAM Structure of the SAM of 1

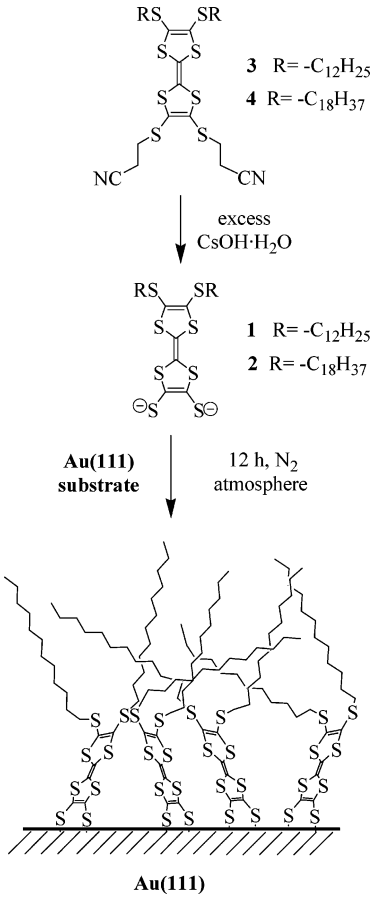

† In memory of Dr. Norma Agnes Stoddart.

* To whom correspondence should be addressed. E-mail: amabilino@icmab.es (D.B.A.); stuart.lindsay@ASU.edu (S.M.L.).

‡ Institut de Ciència de Materials de Barcelona.

|| Arizona State University.

⊥ Present address: National Institute of Standards and Technology, Gaithersburg, MD 20899.

10.1021/jp0495949 CCC: $27.50
Published on Web 04/29/2004

Experimental Section

Synthesis. The TTF derivatives **1** and **2** were prepared as thiolates by deprotecting **3** and **4** (Scheme 1) in situ following the method developed by Becher and co-workers[24,25] by the addition of an excess of cesium hydroxide monohydrate (Aldrich) dissolved in degassed absolute ethanol and stirring for 10 min prior to the substrate immersion (Scheme 1). The intermediates **3**[26] and **4**[25] are known compounds and were prepared according to procedures described in the literature.

Monolayer Preparation. All glassware was cleaned using piranha solution (1:3 hydrogen peroxide/sulfuric acid) and was washed with 18.3 MΩ cm water. Epitaxial Au(111) on mica (Molecular Imaging, Phoenix, AZ) was annealed using a reducing H_2 flame to both remove organic contaminants and facilitate reconstruction of the Au(111) surface. Postannealing, the Au(111) surface was immediately transferred to an inert atmosphere where SAMs of the TTF derivatives **1** and **2** were formed by placing the substrate in a 0.6 μM solution of **3** and **4** in particle-free, distilled tetrahydrofuran (THF). Just prior to deposition, **3** and **4** were completely deprotected[24] as described above. The substrate samples were rinsed with fresh THF and toluene and were used immediately.

Ellipsomety. The thickness of the SAMs was measured using a Gaertner L125b Ellipsometer equipped with a 632.8 nm He−Ne laser. The laser beam was 1 mm in diameter impinging on the sample at an incident angle of 70° with respect to the surface normal. The polarizer was set at 45°. The gold substrate was hydrogen flame annealed to produce a contaminant-free reconstructed Au(111) surface immediately prior to ellipsometric baseline measurements to obtain accurate optical constants of the bare gold substrate. The values reported are an average of five repetitions on five to nine spots from two to three samples for each monolayer/blank sample. A refractive index (n) of 1.50 was assumed for the organic films measured.[8,9] The thickness is only *moderately sensitive* to the exact value of n chosen. For example, a change in n from 1.45 to 1.55 (or a change of ∼7%) results in a change of only ∼2.5% in the calculated thickness. Optical ellipsometry has been widely used to determine the average monolayer thickness of films of *n*-alkylthiols.[8,9] We measured the thickness of dodecanethiol (C12S) and eicosanethiol (C20S) SAMs as references prior to our sample data acquisition. The variation of measured thickness was ±1 Å for the *n*-alkylthiol SAMs and ±2 Å for the TTF derivative SAMs.

IR Spectroscopy. Bulk IR spectra of the compounds **3** and **4** in KBr were acquired from the average of four scans using a standard transmission infrared spectrometer (Fourier Perkin-Elmer, Spectrum one) with a resolution of 4 cm^{-1}. Single reflection ATR (attenuated total reflection) IR spectra for the *n*-alkylmonothiol and compounds **1** and **2** SAMs were obtained using a 65° incidence Ge ATR crystal (Harrick Scientific GATR) in a Bruker IFS 66v/s spectrometer. This system uses an MCT detector cooled with liquid nitrogen to collect the reflected light. A KBr beam splitter was used for mid-IR. Spectra were run in a vacuum at <2 mbar pressure and referenced to background spectra previously determined for the crystal under the same conditions. All spectra were collected at a resolution of 4 cm^{-1} over 1024 scans in the 6000−400 cm^{-1} range. The reference gold substrates were H_2 flame annealed immediately prior to the background collection.

Contact Angle Measurements. Advancing water contact angles were measured by growing small sessile drops on the monolayer surface (1−3 mm diameter) from a fused-silica tubing with an inner diameter of 20 μm and driven with a push−pull syringe pump. A Hunt CCD camera with a 7× magnification was used to monitor and record the data. We considered the maximum advancing contact angle defined by Dettre and Johnson[27] as the angle observed in the limit that the drop is advanced quasistatically over a motionless surface. Water used for contact angles was distilled, deionized, and filtered.

TABLE 1: Ellipsometric Thickness and Advancing Contact Angles for TTF Derivatives SAMs of 1 and 2 on Au(111)

SAM		extended molecular length (Å)	obsd thickness[a] (Å)	$\theta(H_2O)$[b]
$(^-S)_2TTF(SC_{12}H_{25})_2$	**1**	25.0[c]	10.5 ± 2.3	92.6 ± 1.3
$(^-S)_2TTF(SC_{18}H_{37})_2$	**2**	32.5[c]	21.1 ± 1.7	94.5 ± 2.0
$HS(CH2)_{11}CH_3$[d]	$C_{12}S$	14.4[e]	15.4 ± 1.2	100.8 ± 1.2
$HS(CH2)_{19}CH_3$[d]	$C_{20}S$	21.9[e]	22.8 ± 1.3	103.4 ± 1.1

[a] Observed ellipsometric thickness. [b] Advancing water contact angle. [c] Calculated length derived from assumption of fully extended all-anti alkyl chain conformation and TTF molecule perpendicular to the gold surface using Hyperchem program. [d] SAMs used as a reference. [e] Calculated length considering an all-anti alkyl chain conformation tilt of 30°.[28]

Scanning Probe Microscopy and Spectroscopy. All STM images were obtained using a PicoSPM with the sample under toluene with electrochemically etched Pt−Ir tips. The operating set point was 12 pA with a tip bias of −1.0 V. For c-AFM experiments, microfabricated Pt-coated silicon cantilevers with a spring constant of 0.35 N/m (www.spmtips.com, CSC11) were used in the contact mode. Measurements were made with a PicoSPM conducting atomic force microscope (Molecular Imaging, Phoenix, AZ), keeping the sample submerged in freshly distilled toluene during measurements. The solvent reduces contamination and minimizes the adhesion between the AFM tip and the sample.

Results and Discussion

Ellipsometric Thickness Measurements. The thickness of dodecanethiol and eicosanethiol SAMs were measured prior to the sample data acquisition, and the values obtained for these samples are in excellent agreement with the literature data (Table 1).[28] The thickness of the SAMs formed by TTF derivatives **1** and **2** were found to be 10.5 and 21.1 Å, respectively (Table 1). These thicknesses are smaller than those expected for a completely extended molecular all-anti alkyl chain conformation directed perpendicularly away from the gold surface. Indeed, the measured thickness for **1** (of 10.5 Å) is actually less than that of the fully extended alkyl chain component, i.e., dodecanethiol whose SAM has a measured thickness of about 15 Å. Because the measured thicknesses for our calibrants match those expected remarkably well, we rule out any underestimation of the SAM thickness. The shorter measured lengths can be understood as the molecules in the assembly being tilted with respect to the gold substrate. Consideration of molecular models gives a likely scenario for the arrangement of **1** and **2** in the SAMs in which the TTF moiety extends away from the surface at an angle (a parallel arrangement is disfavored by the anchor geometry of the disulfide and goes against other evidence presented here) and the alkyl chains attached to the TTF extend away following approximately the same angle so as to prevent void space. We will discuss the packing of the chains in the next section.

IR Measurements. In Table 2 we present the peak positions for C−H stretching modes in $HS(CH_2)_nCH_3$ and in the TTF derivatives in crystalline, solid, and liquid states and in an adsorbed state on gold. The location of the peak frequencies of the $\nu(CH_2)$ modes provides information about the intermolecular

TABLE 2: Peak Positions for $HS(CH_2)_nCH_3$ and TTF Derivatives C−H Stretching Modes in Crystalline, Solid, and Liquid States and Adsorbed at Gold

mode									
struct group	C−H str mode	**3** (in KBr)[a,b]	**4** (in KBr)[a,b]	**1** SAM[b]	**2** SAM[b]	C_8S liquid[c]	$C_{22}S$ crystalline[c]	$C_{12}S$ SAM[b,d]	$C_{20}S$ SAM[b,d]
$-CH_2-$	ν_a	2918	2919	2925	2925	2924	2918	2920	2919
	ν_s	2849	2850	2852	2852	2855	2851	2850	2850
$-CH_3-$	ν_a(ip)	[e]	[e]	2960	2960	[e]	[e]	2964	2962
	ν_a(op)	[e]	[e]	[e]	[e]	2957	2956	[e]	[e]
	ν_s(FR)	[e]	[e]	[e]	[e]	[e]	[e]	[e]	[e]
	ν_s(FR)	[e]	[e]	2872	2871	[e]	[e]	2875	2875

[a] We present solid-state IR data of compounds **3** and **4** instead of compounds **1** and **2** because they are unstable in air.[25] [b] Peak positions are determined as the average of two independent spectra with standard deviation of ± 1 cm^{-1}. [c] Values reported in ref 28 for 1-docosanethiol ($C_{22}S$) and 1-octanethiol (C_8S). [d] SAMs used as a reference. [e] These bands are masked by the $\nu(CH_2)$ bands.

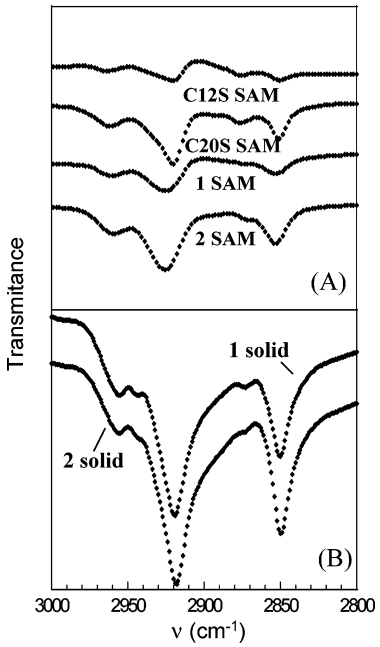

Figure 1. Infrared spectra of (A) self-assembled $HS(CH_2)_nCH_3$ and TTF derivatives on gold and (B) solid TTF derivatives without baseline correction.

environment of the alkyl chains in the SAMs. Porter et al.[28] showed that the locations of these peaks are sensitive to the extent of the lateral van der Waals interactions between long *n*-alkyl chains of *n*-alkylmonothiol monolayers on gold. The peak positions for assemblies of *n*-alkylmonothiol with long alkyl chains (longer than decanethiol) corresponded to those of the bulk crystalline phase, whereas the peak position for *n*-alkylmonothiol with shorter alkyl chains approached that for the pure liquid as a result of a more disordered structure in the monolayers. Our infrared measurements of *n*-alkylmonothiol monolayers reproduce these results, and the TTF derivative SAMs show a similar trend for these peak frequencies (Figure 1). The peak position for the $\nu_a(CH_2)$ mode of monolayers of compounds **1** and **2** are higher than the values obtained for the corresponding solid state spectra of the compounds and lie closer to the value obtained for liquid state *n*-alkylmonothiols. We observe the same tendency for the $\nu_s(CH_2)$ stretching. These data suggest a disordered or liquidlike packing environment in the monolayer[16] and are consistent with the ellipsometric results, and they give the idea of a disordered packing of the alkyl chains which cannot adopt coparallel arrangements because of the steric constraints at the dithio unit at the head of the TTF core. The peak assignment of the other bands in the infrared spectra of monolayers of **1** and **2** are in excellent agreement with previous reports.[16]

Contact Angle Measurements. Table 1 contains the results of advancing contact angle measurements for $C_{12}S$ and $C_{20}S$ monolayers on gold using water as a contacting medium. The measured advancing water contact angles for these *n*-alkylmonothiol monolayers are 100.8° and 103.4°, respectively. These values are somewhat smaller than those reported in the literature.[29−31] The discrepancy between the two could be due to the differences between sample preparation and the difficulties in interpreting advancing contact angles. However, we broadly observe the expected trends. Bain et al.[30] observed consistent advancing water contact angles of ∼110° for *n*-alkanethiol monolayers ($CH_3(CH_2)_nSH$) with $n > 5$ and they noted a marked dropoff in the contact angles when $n < 5$, indicating either that the probe liquid sensed the underlying gold or that an increased disorder was present in the short-chain monolayers. In the case of the monolayers **1** and **2**, we observe advancing water contact angles of 92.6° and 94.5°, respectively. These lower values relative to those for the alkanethiol monolayers are a further indication of a disordered or liquidlike packing of the alkyl chains in the TTF SAMs.

Scanning Probe Microscopy. Both STM and AFM can provide a direct image of the structure of monolayers at the molecular or even atomic scale. In the common with the monolayers formed by *n*-alkanethiols, single Au atom deep terraces and pitlike defects were found for the SAMs of compounds **1** (Figure 2 A−C) and **2** (not shown). Terraces are decorated with a large number of pitlike defects (also called vacancy islands). These pits are typically one Au atom deep but are of variable widths and shapes (Figure 2A−C). The pits observed in alkanethiol SAMs display similar characteristics: depths are sharply centered on 2.5 Å (1 Au atom is 2.88 Å), while the variation in the pit diameters is large, and the shape is typically circular. The irregularity in shape of the pits in the TTF SAMs has been observed in TTF SAMs before[18] and attributed to the liquidlike packing of the chemisorbed molecules.[18] It should be noted that the high density of defects is proportional to the number of molecular domains[32] and is further proof of the disorder (although these defects constitute disorder of a different kind). Figure 2C shows a constant-current STM image of 25×50 nm^2 area of a monolayer of **1** in which bright points are observed with dimensions consistent with individual molecules.

Conducting AFM images obtained for monolayers of **1** are consistent with the STM images (Figure 3). While the topography shows the relatively poor resolution expected for contact mode measurements and the kind of tip employed, current images show a conducting monolayer with an electronic morphology very similar to that observed for this monolayer by STM, with a grainy texture.

Scanning Probe Spectroscopy. The interpretation of measurements of currents through SAMs of the type described here

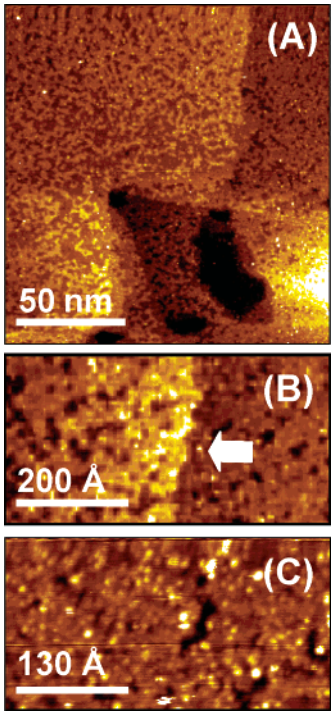

Figure 2. (A) Constant-current 200 × 200 nm^2 area STM images (tunneling current = 12 pA, sample bias voltage = −1.0 V) of a SAM of **1**. (B) A 40 × 75 nm^2 zoom-in from (A) that shows one Au atom step (white arrow). (C) A 25 × 50 nm^2 zoom showing higher resolution.

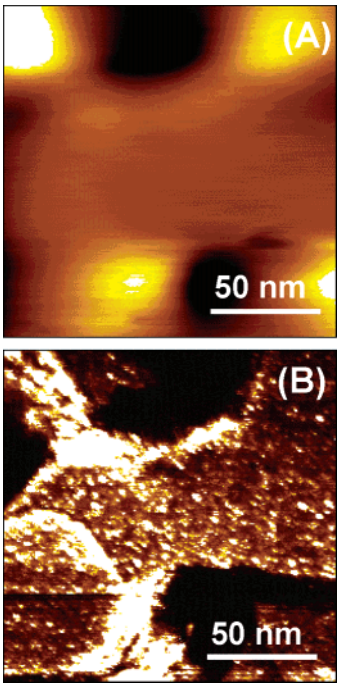

Figure 3. Constant-force 200 × 200 nm^2 area showing simultaneously acquired (A) topography and (B) current measured on a SAM of **1** using a Pt-coated AFM tip.

are generally more complex when compared with measurements on single molecules (for example by attaching nanoparticles to dithiols as described by Cui et al.[33]) This complexity is in part due to the lack of knowledge of the exact number of molecules of the SAM contacted by the tip, and also because of the role of stress in the measured currents. Both these effects are generally correlated, and a careful measurement (especially of the latter effect) is important for meaningful interpretation of data. The contact force dependence of the measured current has

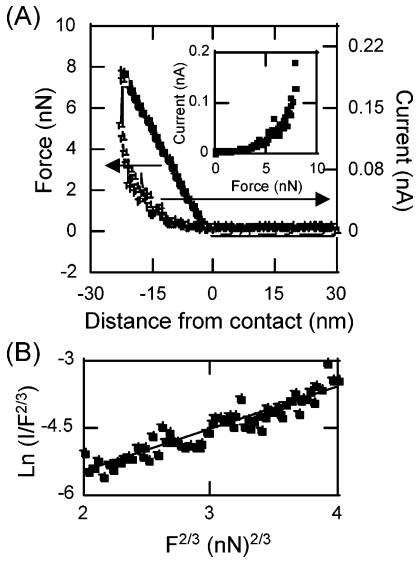

Figure 4. (A) Current and force measured as a conducting AFM cantilever is moved toward a SAM of **1** formed on the Au(111) surface. Nominal contact is achieved at zero distance (0 nm). Negative values imply continued motion toward the Au(111) interface (increasing force). The inset shows the direct relation between current and force. (B) Plot that shows the linear relation between $\ln(I/F^{2/3})$ and $F^{2/3}$, where I is current and F is force.

been studied for monolayers of compound **1**, and we describe the procedure and the analysis below. Currents were recorded simultaneously and independently along with tip displacement as the tip was pushed into a monolayer of **1** on Au(111). Data were taken at a fixed bias with the samples in toluene under argon. In AFM, the deflection of the tip is a direct measure of the contact force. The measured deflection was converted to a force using the spring constant of the cantilever and the deflection signal (Figure 4A). The force "curve" has the typical shape: zero force experienced between the tip and the sample at large separations, a sudden discontinuous "snapping" at contact, followed by a linear region where the probe is pushed rigidly up with the sample. The slope in this region is essentially unity (tip displacement = sample displacement), but there is a small (subnanometer) change in the film thickness as it deforms under the applied stress. The deformation of a film under a contact force can be characterized using the Hertzian model[34] that describes a spherical tip of radius R indenting into a uniform elastic film. The contact radius, r, depends on the force, F, according to

$$r = [FR/K]^{1/3} \tag{1}$$

where K is an effective modulus given by

$$K^{-1} = (3/4)[(1 - \nu_1^2)/E_1 + (1 - \nu_2^2)/E_2] \tag{2}$$

E_1 is the Young's modulus for the monolayer (10^{10} N/m^2)[35] and E_2 is the modulus for the tip (1.7×10^{11} N/m^2).[34] ν_1 and ν_2 are the Poisson ratios for the materials, and we assume them to be 0.33. This leads to a value of $K = 1.4 \times 10^{10}$ N/m^2. The effective spring constant of the film is given by Kr so that deformation, δz, is given by $F/(Kr)$ or

$$\delta z = F^{2/3}/(K^{2/3}R^{1/3}) \tag{3}$$

The tunneling current (I) is proportional to the contact area multiplied by $\exp(-\beta(z-\delta z))$ so that its force dependence is given by

$$I \propto F^{2/3} \exp(CF^{2/3}) \quad (4)$$

where

$$C = [\beta_s/(K^{2/3}R^{1/3})] \quad (5)$$

Thus, the slope from a plot of $\ln(I/F^{2/3})$ and $F^{2/3}$ should be a direct measure of C in this model. A measure of C enables us to determine β_s, which represents the change in tunnel current with change in the dimension of a compressible gap filled with the molecular material. (This number is *not* the same as the electronic decay constant for through-bond tunneling.) Fits to the data for the monolayer of **1** are shown in Figure 4B showing a linear regression ($R_{fit} = 0.94$) in agreement with the theory described in this paragraph resulting in a value of $C = 0.96$ $(nN)^{-2/3}$. The β_s calculated from this value of C considering a tip radius (R) of ~20 nm is 1.5 $Å^{-1}$. This value is larger than those for SAMs formed by alkanethiols, probably as a result of both the mechanical and electrical properties of the monolayers discussed here which incorporate both rigid aromatic sections and alkyl chains.

We have also measured the current−voltage curves by lowering the platinum-coated c-AFM probe onto different spots of the monolayer **1**, and recording the current as the probe bias was swept (typically at a rate of 1 V/s). Both the sweep rate and the range of the sweep were varied to ensure that reproducible data were obtained and that the data were free from hysteresis. A maximum bias of slightly over ±1 V could be applied without bias-dependent changes of the current−voltage characteristics from sweep to sweep, and measurements were made only up to ±1 V. All the $I(V)$ curves recorded in different spots for forces between 4 and 5 nN have essentially the same shape, although the variations in the absolute magnitude of the currents were relatively large and lead to large standard deviations. It is important to appreciate that because $I(V)$ data are collected from a combination of several tips on different spots on the sample, and although the forces are controlled, small force instabilities (for example, due to charging during a bias sweep) are inevitable. The resulting variability is difficult to control or monitor and typically results in a large standard deviation, especially when SAMs are touched with the AFM tip (Figure 5).

A readily observable feature of the conductance spectra is the smooth asymmetry (Figure 5) which arises from (a) the inherent asymmetry of the junction because the metals contacting the molecule at the ends are different−covalent gold at the substrate side and a platinum tip contacting noncovalently at the other end−and (b) the junction contains regions that are thinner or wider than the average thickness (10.5 Å) due to "disorder" or "fluidity" in the SAM formed from **1**, as highlighted earlier.

The $I(V)$ curve presented in Figure 5A is the average of 55 measurements in different areas of the monolayers in the range of force between 4 and 5 nN. Below, we describe how we calculate the resistance through a single molecule in a SAM of **1**. Considering an average contact force of 4 nN and a tip radius (R) of ~20 nm (a conservative estimate according to electron microscopy measurements), we can determine a contact radius (r) of 1.8 nm using eq 1. This value corresponds to a tip area of 10.1 nm^2. The distance between the two thiol groups attached to the TTF unit is 0.33 nm, corresponding to an area per molecule of 0.34 nm^2. Using these values for the tip area and area per molecule and assuming close packing (to give a lower limit for the conductance), we then would have approximately 30 molecules under the tip. Dividing the averaged curve (Figure 5A) by 30, we obtain a new curve with an ohmic region ($R_{fit} = 0.999$) with a resistance of $(25.7 \pm 0.3) \times 10^9$ Ω (Figure 5B). This corresponds to the resistance of a single molecule in a SAM of **1**. This estimate contrasts with measurements where the resistances are determined on single molecules.[33]

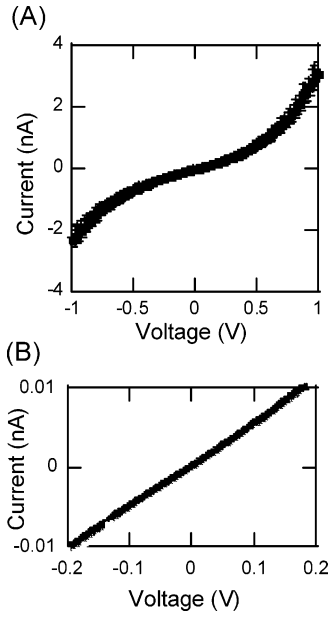

Figure 5. (A) The curve shown is 4% of the points of an average of 55 $I(V)$'s recorded with the tip contacting different spots of SAMs of **1** for two samples (the standard error is shown). (B) From the ohmic region, low-bias region, the resistance of a molecule of **1** is determined to be 25.7 ± 0.3 GW.

TTF SAMS vs "Molecular Wires". Before analyzing how the TTF molecules compare both with other candidate molecular wires and with an ideal quantum wire, it is important to appreciate a few different methodologies by which measurements are typically made. With the two-terminal geometry possible with the c-AFM, there are two different routes to address the electrical characteristics of individual molecules. The first, as we have described here, measures the properties of an ensemble of molecules with a clear dependence of current on the force; this is described as a "mechanical contact". Alternately, isolating or inserting a dithiol in an insulating SAM and chemically attaching a nanoparticle to the free thiol end of the dithiol species results in a large area contact pad with which the molecule can be addressed.[33] Because the area of the dithiol plus nanoparticle system is relatively large (compared with a single molecule in a SAM), and because a metal−metal bond can be formed between the c-AFM tip and the nanoparticle, these experiments tend to selectively measure the electrical characteristic of a single (or a few) molecules at one time.[33] In general, the measured current is independent of the applied force as well. c-AFM measurements on dithiols with nanoparticles attached are thus described as measurements with "covalent or chemical contacts". An important difference between measurements made with mechanical and covalent contacts is that the measured currents are much larger in the latter, underlining the pivotal role played by the interface in electron transport at the nanoscale (contact resistance is an important parameter in the bulk as well). As an example, the resistance of octanedithiol is 900 ± 50 MΩ,[36] which is at least 4 orders of magnitude less resistive than the analogous octane monothiol.[37] Resistances measured with covalent contacts for carotenedithiol[38] and 2,5-di(phenylethynyl-4′-thioacetyl)benzene (TPE)[39] are 4.9 ± 0.2 and 52 ± 18 GΩ, respectively.[40] The conjugated carotenedithiol (28 carbons atoms) is nearly as long as the TTF molecule **1**,

whereas the TPE molecule contains 16 carbon atoms along its length. First, it is remarkable that the resistance of the TTF molecule **1**, 25.7 ± 0.3 GΩ, is between these two values despite its hypothetical molecular length (25 Å). This value represents a very large conductance, especially for a molecule with mechanical contacts. All data presented indicate that the molecules of **1** are loosely packed in the SAM and that both the alkanethiol chains attached to the main TTF skeleton and the aromatic cores themselves are not perpendicular but tilted with respect to the normal to the Au(111) surface, and there is an essentially fluidlike and nonuniform alkyl chain coating. Thus, the metal-coated c-AFM tip may almost directly contact the bulk of the TTF unit, which in any case is not perpendicular to the surface, resulting in the large currents observed.

Conclusions

The monolayers of molecules of **1** and **2** which are linked to a Au(111) surface through a 1,2-ethylene dithiolate residue pack spontaneously on Au(111), although the packing in lateral dimensions is not dense because of the lack of favorable interactions between the alkyl chains. This is the first time, to our knowledge, that this type of moiety has been used as a binding unit for a gold surface. c-AFM measurements allowed us to estimate the resistance of a single molecule of **1** as 25.7 ± 0.3 GΩ, which is remarkably conductive for an organic molecule with mechanical contacts. The TTF unit itself is relatively short and is comparable to the length of 1-octanethiol or ∼11 Å. The measured resistance through 1-octanethiol monolayers is ≫100 GΩ,[37] with an exact determination limited at very low currents by noise; this clearly indicates that the TTF unit itself is an excellent medium for electron transport. On the basis of these observations, we suggest that the dithiol variants of **1** would be ideal as candidate molecular wires,[41] in the type of SAMs described here, or in other self-assembled systems.[42,43]

Acknowledgment. This work was supported by grants from the DGI, Spain (Project No. BQU 2003-00760), DGR, Catalonia (Project No. 2001SGR00362), and the NSF NIRT (ECS 01101175). E.G.-N. thanks the Generalitat de Catalunya for a predoctoral and travel grant, and Timothy Karcher, Shawn Whaley, and Brian Ashcroft for their kind help in ellipsometric, infrared, and contact angle measurements, respectively.

References and Notes

(1) Joachim, C.; Gimzewski, J. K.; Aviram, A. *Nature* **2000**, *408*, 541−548.
(2) Tour, J. *Acc. Chem. Rev.* **2000**, *33*, 791−804.
(3) Kovtyukhova, N. I.; Mallouk, T. E. *Chem. Eur. J.* **2002**, *8*, 4354−4363.
(4) Carroll, R. L.; Gorman, C. B. *Angew. Chem., Int. Ed.* **2002**, *41*, 4378−4400.
(5) Fan, F.-R.; Yang, J.; Cai, L.; Price, D. W.; Shawn, J.; Dirk, M.; Kosynkin, D. V.; Yao, Y.; Rawlett, A. M.; Tour, J. M.; Bard, A. J. *J. Am. Chem. Soc.* **2002**, *124*, 5550−5560.
(6) Armstrong, F. A.; Wilson, G. S. *Electrochim. Acta* **2000**, *45*, 2623−2645.
(7) Zhang, J.; Grubb, M.; Hansen, A.; Kuznetsov, A. M.; Boisen, A.; Wackerbarth, H.; Ulstrup, J. *J. Phys.: Condens. Matter* **2003**, *15*, S1873−S1890.
(8) Ulman, A. *An Introduction to Ultrathin Organic Films from Langmuir−Blodgett to Self-Assembly*; Academic Press: New York, 1991.
(9) Schreiber, F. *Prog. Surf. Sci.* **2000**, *65*, 151−256.
(10) Nielsen, M. B.; Lomholt, C.; Becher, J. *Chem. Soc. Rev.* **2000**, *29*, 153−164.
(11) Segura, J. L.; Martín, N. *Angew. Chem., Int. Ed.* **2001**, *40*, 1372−1409.
(12) Farges, J.-F. *Organic Conductors: Fundamentals and Applications*; Marcel Dekker: New York, 1994.
(13) Williams, J. M.; Ferraro, J. R.; Thorn, R. J.; Carlson, K. D.; Geiser, U.; Wang, H. H.; Kini, A. M.; Whangbo, M.-H. *Organic Superconductors (Including Fullerenes) Synthesis, Structure, Properties, and Theory*; Prentice Hall: Englewood Cliffs, NJ, 1992.
(14) Jeppesen, J. O.; Nielsen, K. A.; Perkins, J.; Vignon, S. A.; Di Fabio, A.; Ballardini, R.; Gandolfi, M. T.; Venturi, M.; Balzani, V.; Becher, J.; Stoddart, J. F. *Chem. Eur. J.* **2003**, *9*, 2982−3007.
(15) Tseng, H.-R.; Vignon, S.; Stoddart, J. F. *Angew. Chem., Int. Ed.* **2003**, *42*, 1491−1495.
(16) Yip, C.; Ward, M. D. *Langmuir* **1994**, *10*, 549−556.
(17) Moore, A. J.; Goldenberg, L. M.; Bryce, M. R.; Petty, M. C.; Monkman, A. P.; Marenco, C.; Yarwood, J.; Joyce, M. J.; Port, S. N. *Adv. Mater.* **1998**, *10*, 395−398.
(18) Ryota, Y.; Akira, M.; Toshiaki, E.; Eisuke, I.; Fumio, N.; Masahiko, H. *Mol. Cryst. Liq. Cryst.* **2001**, *370*, 273−276.
(19) Liu, S.-G.; Liu, H.; Bandyopadhyay, K.; Gao, Z.; Echegoyen, L. *J. Org. Chem.* **2000**, *65*, 3292−3298.
(20) Fibbioli, M.; Bandyopadhyay, K.; Liu, S.-G.; Echegoyen, L.; Enger, O.; Diederich, F.; Gingery, D.; Bühlmann, P.; Persson, H.; Suter, U. W.; Pretsch, E. *Chem. Mater.* **2002**, *14*, 1721−1729.
(21) Campuzano, S.; Gálvez, R.; Pedrero, M.; Manuel de Villena, F. J.; Pingarrón, J. M. *J. Electroanal. Chem.* **2002**, *526*, 92−100.
(22) Herranz, M. A.; Yu, L.; Martín, N.; Echegoyen, L. *J. Org. Chem.* **2003**, *68*, 8379−8385.
(23) Dahlstedt, E.; Hellberg, J.; Petoral, R. M.; Uvdal, K. *J. Mater. Chem.* **2004**, *14*, 81−85.
(24) Svenstrup, N.; Rasmussen, K. M.; Hansen, T. K.; Becher, J. *Synthesis* **1994**, 809−812.
(25) Simonsen, K.; Svenstrup, N.; Lau, J.; Simonsen, O.; Mork, P.; Kristensen, G. J.; Becher, J. *Synthesis* **1996**, 407−418.
(26) Abdel-Mottaleb, M. M. S.; Gomar-Nadal, E.; De Feyter, S.; Veciana, J.; Rovira, C.; Amabilino, D. B.; De Schryver, F. Manuscript in preparation.
(27) Dettre, R. H.; Johnson, R. E. *J. Phys. Chem.* **1965**, *69*, 1507−1515.
(28) Porter, M. D.; Bright, T. B.; Allara, D. L.; Chidsey, C. *J. Am. Chem. Soc.* **1987**, *109*, 3559−3568.
(29) Troughton, E. B.; Bain, C. D.; Whitesides, G. M.; Nuzzo, R. G.; Allara, D. L.; Porter, M. D. *Langmuir* **1988**, *4*, 365−385.
(30) Bain, C. D.; Troughton, E. B.; Tao, Y.-T.; Evall, J.; Whitesides, G. M.; Nuzzo, R. G. *J. Am. Chem. Soc.* **1989**, *111*, 321−335.
(31) Laibinis, P. E.; Whitesides, G. M.; Allara, D. L.; Tao, Y.-T.; Parikh, A. N.; Nuzzo, R. G. *J. Am. Chem. Soc.* **1991**, *113*, 7152−7167.
(32) Poieir, G. E. *Chem. Rev.* **1997**, *97*, 1117−1128.
(33) Cui, X. D.; Primak, A.; Zarate, X.; Tomfohr, J.; Sankey, O. F.; Moore, A. L.; Moore, T. A.; Gust, D.; Harris, G.; Lindsay, S. M. *Science* **2001**, *294*, 571−574.
(34) Burnham, N. A.; Colton, R. J. *J. Vac. Sci. Technol., A* **1993**, *7*, 2906−2913.
(35) Weihs, T. P.; Nawaz, Z.; Jarvis, S. P.; Pethica, J. B. *Appl. Phys. Lett.* **1991**, *59*, 3536−3538.
(36) Cui, X. D.; Primak, A.; Zarate, X.; Tomfohr, J.; Sankey, O. F.; Moore, A. L.; Moore, T. A.; Gust, D.; Nagahara, L. A.; Lindsay, S. M. *J. Phys. Chem. B* **2002**, *106*, 8609−8614.
(37) Cui, X. D.; Zarate, X.; Tomfohr, J.; Sankey, O. F.; Primak, A.; Moore, A. L.; Moore, T. A.; Gust, D.; Harris, G.; Lindsay, S. M. *Nanotechnology* **2002**, *13*, 5−14.
(38) Ramchandran, G. K.; Tomfohr, J. K.; Li, J.; Sankey, O. F.; Zarate, X.; Primak, A.; Terazano, Y.; Moore, T. A.; Moore, A. L.; Gust, D.; Nagahara, L. A.; Lindsay, S. M. *J. Phys. Chem. B* **2003**, *107*, 6162−6169.
(39) Wold, D. J.; Haag, R.; Rampi, M. A.; Frisbie, C. D. *J. Phys. Chem. B* **2002**, *106*, 2813−2816.
(40) For a review giving comparisons of conduction through molecules, see: Salomon, A.; Cahen, D.; Lindsay, S.; Tomfohr, J.; Engelkes, V. B.; Frisbie, C. D. *Adv. Mater.* **2003**, *15*, 1881−1890.
(41) Gautier, N.; Dumur, F.; Lloveras, V.; Vidal-Gancedo, J.; Veciana, J.; Rovira, C.; Hudhomme, P. *Angew. Chem., Int. Ed.* **2003**, *42*, 2765−2768.
(42) Gomar-Nadal, E.; Abdel-Mottaleb, M. M. S.; De Feyter, S.; Veciana, J.; Rovira, C.; Amabilino, D. B.; De Schryver, F. C. *Chem. Commun.* **2003**, 906−907.
(43) Abdel-Mottaleb, M. M. S.; Gomar-Nadal, E.; De Feyter, S.; Zdanowska, M.; Veciana, J.; Rovira, C.; Amabilino, D. B.; De Schryver, F. C. *Nano Lett.* **2003**, *3*, 1375−1378.